1   **Direct reprogramming of human fibroblasts into insulin-producing cells**

2   **by transcription factors**

3

4   **Running title:** Reprogramming of fibroblasts to insulin-producing cells

5

6   Marta Fontcuberta-PiSunyer[1,2], Ainhoa García-Alamán[1,3], Èlia Prades[1], Noèlia

7   Téllez[3,4,5], Hugo Figueiredo[1,2], Rebeca Fernandez-Ruiz[1,3], Sara Cervantes[1,3], Carlos

8   Enrich[1,2], Laura Clua[6], Javier Ramón-Azcón[6], Christophe Broca[7], Anne Wojtusciszyn[7,8],

9   Anna Novials[1,2], Nuria Montserrat[6,9,10], Josep Vidal[1,2,3,11], Ramon Gomis[1,2,3,12], Rosa

10   Gasa[1,3] *

11

12   [1] Institut d'Investigacions Biomèdiques August Pi i Sunyer (IDIBAPS), Barcelona, Spain

13   [2] Faculty of Medicine and Health Sciences, Universitat de Barcelona, Barcelona, Spain

14   [3] Centro de Investigación Biomédica en Red de Diabetes y Enfermedades Metabólicas

15   Asociadas (CIBERDEM), Spain

16   [4] Institut d'Investigació Biomèdica de Bellvitge (IDIBELL), Barcelona, Spain

17   [5] Biosciences department, University of Vic - Central University of Catalonia (UVic-

18   UCC), Vic, Spain

19   [6] Institute for Bioengineering of Catalonia (IBEC), The Barcelona Institute of Technology

20   (BIST), Barcelona, Spain

21   [7] CHU Montpellier, Laboratory of Cell Therapy for Diabetes (LTCD), Hospital St-Eloi,

22   Montpellier, France

23   [8] Service of Endocrinology, Diabetes and Metabolism, Lausanne University Hospital,

24   Lausanne, Switzerland

25   [9]Centro de Investigación Biomédica en Red en Bioingeniería, Biomateriales y

26   Nanomedicina, Madrid, Spain

27   [10]Catalan Institution for Research and Advanced Studies (ICREA), Barcelona, Spain

28   [11]Endocrinology and Nutrition Department, Hospital Clinic of Barcelona, Barcelona,

29   Spain

30   [12]Universitat Oberta de Catalunya (UOC), Barcelona

31

32   *corresponding author and lead contact

33   rgasa@clinic.cat

34

35

36

37

38

39

40

41

42

43

44

45   **ABSTRACT**

46   Direct lineage reprogramming of one somatic cell into another bypassing an

47   intermediate pluripotent state has emerged as an alternative to embryonic or induced

48   pluripotent stem cell differentiation to generate clinically relevant cell types. One cell

49   type of clinical interest is the pancreatic β cell that secretes insulin and whose loss

50   and/or dysfunction leads to diabetes. Generation of functional β-like cells from

51   developmentally related somatic cell types (pancreas, liver, gut) has been achieved via

52   enforced expression of defined sets of transcription factors. However, clinical

53   applicability of these findings is challenging because the starting cell types are not

54   easily obtainable. Skin fibroblasts are accessible and easily manipulated cells that

55   could be a better option, but available studies indicate that their competence to give

56   rise to β cells through similar direct reprogramming approaches is limited. Here, using

57   human skin fibroblasts and a protocol that ensures high and consistent expression of

58   adenovirus-encoded reprogramming factors, we show that the transcription factor

59   cocktail consisting of Pdx1, Ngn3, MafA, Pax4 and Nkx2-2 activates key β cell genes

60   and down-regulates the fibroblast transcriptional program. The converted cells produce

61   insulin and exhibit intracellular calcium responses to glucose and/or membrane

62   depolarization. Furthermore, they secrete insulin in response to glucose *in vitro* and

63   after transplantation *in vivo*. These findings demonstrate that transcription factor-

64   mediated direct reprogramming of human fibroblasts is a feasible strategy to generate

65   insulin-producing cells.

66

67

68

69

70 **INTRODUCTION**

71

72 The discovery that adult somatic cells can be reprogrammed into induced pluripotent

73 stem cells (iPSC) [1, 2] has revolutionized current biological and medical research.

74 Human iPSC can provide valuable platforms for drug and toxicology screens, for

75 investigating human development and for disease modeling. Furthermore, the

76 possibility of differentiating iPSC into clinically relevant cell types for autologous cell

77 therapy has pushed the field of regenerative medicine forward. However, current iPSC

78 technology is still technically demanding, expensive, time consuming and produces

79 cells of variable quality. Similarly, design of the *in vitro* differentiation protocols to

80 generate specific cell types is not trivial. Recapitulation of in vivo developmental

81 pathways using signaling molecules is considered the most effective approach, but

82 defining and adjusting proper in vitro differentiation conditions is not a straightforward

83 task, and differentiation protocols are often long and expensive, present poor

84 reproducibility and have variable efficiencies among laboratories.

85

86 An alternative strategy to produce cell types of interest is direct lineage reprogramming,

87 which entails the direct conversion of one differentiated cell type into another bypassing

88 an intermediate pluripotent stage. This strategy is often based on the forced expression

89 of cocktails of transcription factors (TF) that normally function as potent fate

90 determinants of the cell type of interest in development [3-5]. This approach presents

91 several advantages over pluripotent cell derivation including its relative simplicity and

92 speed (fewer induction steps) and, in terms of translational potential, its safety due to

93 avoidance of the tumorigenic risk associated with pluripotency [6]. Moreover, as with

94 iPSC, this strategy allows autologous transplantation thus eluding the problem of

95 allograft rejection.

96

97 Pancreatic beta   (β) cells produce insulin, which controls whole body glucose

4

98   homeostasis. Relative or complete deficit of functioning β cells is a hallmark of diabetes

99   and thus β-cell replacement has emerged as a promising therapeutic approach to treat

100   and eventually cure this disease. To date, derivation of β-cells from pluripotent

101   (embryonic and iPS) cells has been intensively studied, with significant progress made

102   during the past fifteen years [7-11]. Yet, current protocols are still on the way of

103   standardization and face important challenges including low number and functional

104   maturation of generated β-like cells [12, 13]. Direct lineage reprogramming strategies to

105   create β-cells bypassing the iPSC stage have also been explored. In this line, the

106   Melton laboratory developed the first TF-based *in situ* conversion of mouse pancreatic

107   exocrine cells towards insulin-producing cells through expression of three TFs: Pdx1,

108   Ngn3 and MafA (hereafter PNM)[14]. Subsequently, these factors, individually or

109   combined, have been shown to promote β-cell-like features in related endodermal cell

110   lineages such as pancreatic ductal cells, hepatic, intestinal or stomach cells [15-21].

111

112   One central aspect in direct reprogramming approaches, particularly when considering

113   their clinical applicability, is the choice of cell source. Ideally, the starting material

114   should be accessible, easy to handle/grow and susceptible to reprogramming. To date

115   fibroblasts, which can be readily obtained from small skin biopsies, are commonly used

116   as cell source for IPSC generation. Remarkably, they have also been directly

117   reprogrammed towards somatic cell types including cardiomyocytes [22], chondrocytes[23],

118   neurons [24] or oligodendrocyte progenitors [25]. In the pancreas field, human fibroblasts

119   have been converted into expandable pancreatic progenitor populations through

120   transient overexpression of iPSC factors in conjunction with lineage-determining

121   soluble factors [26] and into insulin-producing cells following long protocols that are

122   reminiscent of the small molecule-based directed differentiation procedures applied to

123   stem cells [26-28]. However, attempts to use cell-specific TFs to directly transform

124   fibroblasts into β cells have yielded discouraging results [14, 20, 29, 30].

125

126   The growing potential of direct lineage reprogramming to generate specialized cell

127   types, the medical interest in pancreatic β cells and the prevailing challenges for the

128   generation of these cells via conventional directed differentiation from pluripotent cells,

129   prompted us to examine the amenability of fibroblasts to be reprogrammed to β cells

130   using cell-specific transcription factors in a more comprehensive manner. Here we

131   show that the combination of five endocrine TF induces activation of the β-cell

132   transcriptional program in human fibroblasts. Furthermore, we show that

133   reprogrammed fibroblasts produce and secrete insulin *in vitro* and *in vivo*. We believe

134   these findings demonstrate the feasibility of this approach and set the basis to explore

135   this path for generation of insulin-producing cells for disease modeling and cellular

136   therapy.

137

138   **MATERIALS and METHODS**

139

140   **Fibroblasts**

141   Human foreskin fibroblasts were prepared from a foreskin biopsy from a 3-year old

142   individual after obtaining his parents' written informed consent (HFF1). Adult human

143   dermal fibroblasts were prepared from arm biopsies of two T1D individuals after

144   obtaining their written informed consent (HDF-DT1-1, HDF-DT1-2). In brief, skin

145   samples were collected in sterile saline solution, divided into small pieces, and allowed

146   to attach to cell culture dishes before adding Iscove's modified Dulbecco's medium

147   (Invitrogen, Carlsbad, CA, USA) supplemented with 10% human serum (Sigma, St.

148   Louis, MO, USA) and penicillin/streptomycin (0.5X) (Invitrogen). After 10 days of

149   culture at 37°C, 5% CO_2, fibroblast outgrowths were dissociated and split 1:4 using a

150   recombinant trypsin-like enzyme (TrypLE Select, Invitrogen). Additional fibroblast

151   preparations were commercially available: HFF2 (SCRC1041[TM], ATCC, Manassas, VA,

152   USA) and HDF-1 (PCS-201-012, ATCC) and HDF-2 (Cell Applications, San Diego, CA,

153   USA).

154

Human islets

156 Human islets were prepared by collagenase digestion followed by density gradient

157 purification at the Laboratory of Cell Therapy for Diabetes (Hospital Saint-Eloi,

158 Montpellier, France), as previously described [31]. After reception in Barcelona, human

159 islets were maintained in culture for 1-3 days in RPMI-1640 with 5.5mM glucose, 10%

160 fetal bovine serum (FBS) and antibiotics, before performing the experiments.

161 Experiments were performed in agreement with the local ethic committee (CHU,

162 Montpellier) and the institutional ethical committee of the French Agence de la

163 Biomédecine (DC Nos. 2014-2473 and 2016-2716). Informed consent was obtained for

164 all donors.

165

Recombinant adenoviruses

167 The adenoviral expression vector pAd/CMV/V5-DEST carrying mouse Pdx1, Ngn3,

168 MafA and 2A-Cherry under the CMV promoter was kindly provided by Dr. Q. Zhou,

169 Harvard University[29]. The recombinant adenovirus (termed Ad-PNM) was generated

170 after Pac1 digestion and transfection into HEK293 cells. The recombinant adenovirus

171 encoding Pdx1 was kindly provided by the Beta Cell Biology Consortium. The

172 recombinant adenovirus encoding MafA was purchased from Vector Biolabs (Chicago,

173 IL, USA). All other recombinant adenoviruses encoding single transcription factors

174 (Ngn3, NeuroD1, Nkx2.2, Nkx6.1 and Pax4) were described previously[18, 32].

175

Reprogramming protocol

177 Fibroblasts were grown in DMEM media supplemented with 10% (v/v) fetal bovine

178 serum (FBS), 100 U/ml penicillin, 100 µg/ml streptomycin and 1% Glutamax. They

179 were plated onto 96-well plates (9 500 cells per well) for MTT and BrdU assays, onto

180 12-well plates (1.25×10^5 cells/well) for gene expression, insulin secretion,

181 immunofluorescence and caspase assays and onto 10 cm plates (1.5×10^6 cells/plate)

182   for transplantation experiments. Infection with Ad-PNM was performed when fibroblasts

183   reached 80% confluence, normally 1-2 days after seeding. In brief, for 12-well plates,

184   fibroblasts were incubated with 0.6ml complete culture medium containing Ad-PNM at

185   a dose of 15 moi (multiplicity of infection) for 16-20 h. After virus removal, media was

186   changed to RPMI-1640 medium containing 6% FBS and antibiotics. Two and five days

187   after incubation with Ad-PNM, fibroblasts were infected for 6-8 h with Ad-Pax4 (50 moi)

188   and Ad-Nkx2.2 (50 moi) respectively. The transfection reagent Superfect (Qiagen,

189   Venlo, Netherlands) was always added to the virus-containing media in order to

190   achieve efficient adenoviral infection and transgene expression in fibroblasts. Amounts

191   were scaled down or up according to the well size. To prepare spheroids, one day after

192   Ad-Nkx2.2 infection, cells were trypsinized and transferred (1 200-1 800 cells/ well) to

193   96-well Nunclon Sphera plates (Thermo Scientific) for gene expression,

194   immunofluorescence and insulin secretion assays. Cell spheroids (1 000 cells/cluster)

195   for transplantation were generated in AggreWell plates (StemCell Technologies,

196   Saint Égrève, France**)**

197

198   **RNA isolation and reverse transcriptase polymerase chain reaction (RT-PCR)**

199   Total RNA from cultured cells was isolated using NucleoSpin®RNA (Macherey-Nagel),

200   Düren, Germany) following the manufacturer's manual. Total RNA from enucleated

201   eyes was extracted using Trizol reagent (Sigma) and then cleaned and DNAse-treated

202   using RNeasy mini columns (Qiagen) prior to cDNA synthesis. First-strand cDNA was

203   prepared using Superscript III Reverse Transcriptase (Invitrogen) and random

204   hexamers in a total volume of 20 ul and 1/40 to 1/200 of the resulting cDNA was used

205   as a template for real time PCR reactions. Real time PCR was performed on an ABI

206   Prism 7900 detection system using Gotaq master mix (Promega, Madison, WI, USA).

207   Expression relative to the housekeeping gene *TBP* was calculated using the delta(d)Ct

208   method and expressed as $2^{\wedge}(-dCT)$ unless otherwise indicated. Primer sequences are

209   provided in Table S3.

210

BrdU and MTT assays

212 For quantification of cell proliferation, cells in 96-well plates were cultured overnight

213 with medium containing 5-bromo-2'-deoxuridine (BrdU). BrdU incorporation was

214 determined colorimetrically with the Cell proliferation ELISA kit (Roche, Basilea,

215 Switzerland) following the manufacturer's instructions. For assessing cell viability, cells

216 grown in 96-well plates were incubated with medium containing 0.75 mg/ml of 3-(4,5-

217 dimethythiazol-2-yl)-2,5-diphenyltetrazolium bromide (MTT) for 3 hours at 37ºC. The

218 resulting formazan crystals were solubilized in Isopropanol/0.04 N HCl solution and

219 optical density [1] was read at 575 nm and 650 nm using a Synergy HT reader (BIO-TEK

220 Instruments, Winooski, VT, USA). The OD (575-650) was expressed relative to control

221 fibroblasts, which were given the value of 100%.

222

Calcium imaging

224 To study glucose-dependent calcium influx, cells were washed with Hanks' Balanced

225 Salt Solution (HBSS, Sigma) and incubated with Fluo4-AM (Life Technologies) in fresh

226 2.5 mM glucose Krebs-Ringer bicarbonate buffer for 1 hour at 37ºC in the

227 dark. Intracellular calcium fluorescence was recorded from fluo-4-loaded cells using a

228 Leica TCS SPE confocal microscope with an incubation chamber set at 37C, and a 40x

229 oil immersion objective. Fluorescent images and average fluorescence intensity were

230 acquired at 600Hz every 1.8 seconds, using a 488nm excitation laser, an emission set

231 at 520 with a bandwidth of 10nm. Image registry consisted of: 5 min in 2 mM glucose-

232 Krb buffer, 10 min in 22 mM glucose-Krb buffer and 5 min in 30 mM KCl-Krb buffer.

233 Average fluorescence intensity images of each individual cell were analyzed with LAS

234 AF Lite and Fuji programs.

235

In vitro glucose-induced insulin secretion and content

237   Cells in 2D or 3D aggregates were washed with phosphate-buffered saline (PBS) and

238   preincubated for 30-45 min at 37°C in Hepes-buffered Krebs-Ringer buffer with 2mM

239   glucose. Preincubation solution was then removed and cells incubated with the same

240   buffer containing different glucose concentrations glucose for additional 90 min.

241   Supernatants were collected to measure secreted insulin or C-peptide. Cells were

242   lysed in detergent-containing buffer (Tris-HCl pH8 50mM, NaCl 150mM, SDS 0.1%

243   (w/v), Igepal CA-630 1%, Na deoxycholate 0.5%) to determine C-peptide content.

244   Human insulin was measured using a human Insulin ELISA kit (Crystal Chem,

245   Zaandam, Netherlands) and C-peptide using a human C-peptide ELISA kit (Mercodia,

246   Uppsala, Sweden).

247

248   **Electron microscopy**

249   Cell spheroids were collected, washed with PBS and fixed with 4% paraformaldehyde/

250   0.5% glutaraldehyde (Sigma) mixture in 0.1M phosphate buffer (PB) pH7.4 for 30min at

251   4°C and gentle agitation. Cells were then transferred to fresh fixation solution and

252   maintained at 4°C until secondarily fixed with 1% uranyl acetate and 1% osmium

253   tetroxide. Cells were then dehydrated, embedded in Spurr's Resin and sectioned using

254   Leica ultramicrotome   (Leica Microsystems). Conventional transmission electron

255   microscopy (TEM) images were acquired from thin sections using a JEOL-1010

256   electron microscopy equipped with an SC1000 ORIUS-CCD digital camara (Gatan).

257

258   **Transplant procedures**

259   Adult (12-20 week old) immunocompromised NSG-SCID mice (005557, Jackson

260   Laboratories) received implants in the anterior chamber of the eye (ACE),

261   subcutaneously or between the omental sheets as previously described[33, 34]. A total of

262   150-200 human islets, 300 iβ-like cell or HFF1 spheroids (1 200-1 800 cells/cluster)

263   were transplanted per eye and approximately 4000-iβ-like cell spheroids (750-1 000

264   cells/cluster) were transplanted into either of the other two implant sites. For

265 subcutaneous and omental transplants, collagen scaffolds were used. Briefly, the cell-

266 laden collagen hydrogel was prepared by mixing 150 µl of a 4 mg/ml rat tail type I

267 collagen (Corning, NY, USA) solution, prepared following the manufacturer's

268 instructions, with iβ-like cell clusters (pelleted by gentle centrifugation) and poured onto

269 a cylindrical 8 mm diameter x 1 mm thick PDMS mold (Dow Corning Sylgard 184

270 Silicone Elastomer). The hydrogel was polymerized for 20 min at 37 ℃, detached from

271 the mould and maintained in tissue culture dishes with warm RPMI-1640 medium until

272 transplant (usually 2-3 hours). Constructs were introduced in the abdominal

273 subcutaneous space through a small (1–2 mm) incision. Alternatively, constructs were

274 placed on the omentum close to the duodenal-stomack junction and fixed using

275 Histoacryl translucent (Braun, Kronberg im Taurus, Germany). The local ethical

276 committee for animal experimentation of the University of Barcelona approved all

277 animal experiments and procedures.

278

279 **Graft viability and function analysis**

280 To assess vascularization and cell viability in ACE implants, iβ-like clusters were

281 labeled with the long-term tracer for viable cells CFDA (Invitrogen) before

282 transplantation. At day 10 post-transplantation, mice received an intravenous injection

283 of RITC-dextran and in vivo imaging was used to assess functional vascularization and

284 cell viability [34]. For determination of glucose-induced insulin secretion, mice were

285 fasted for 5-6 h and then injected intraperitoneally with glucose (3g/Kg). Aqueous

286 humor from mice with ACE implants was obtained 30 minutes after the glucose

287 challenge and kept frozen until human insulin determination. Tail blood before and after

288 (20 minutes) the glucose challenge was obtained from mice with subcutaneous and

289 omental implants. Human insulin in aqueous humor and in plasma was determined

290 using an ultrasensitive Human Insulin ELISA (Chrystal Chem).

291

292 **Immunofluorescence**

11

293   iβ-like cells grown in 2D were fixed with 4% (v/v) paraformaldehyde (PFA) during 15

294   min and incubated with blocking solution (0.25% (v/v) Triton, 6% (v/v) donkey serum,

295   5% (w/v) BSA in PBS for 1 h at room temperature. Slides were then incubated with

296   primary antibodies diluted in PBS-triton 0.1% (v/v) containing 1% donkey serum

297   overnight at 4 o C. iβ-like cells grown in spheroids were fixed with 4% (v/v)

298   paraformaldehyde (PFA) for 15 min at 4ºC, permeabilized with 0.5% (v/v) Triton in PBS

299   for 20 min and blocked with 0.5% (v/v) Triton/ FBS 10% (v/v) in PBS during 1 h at room

300   temperature. Slides were then incubated with primary antibodies diluted in blocking

301   solution overnight at 4ºC. Eyes were obtained by enucleation, fixed overnight in 2%

302   (v/v) PFA, dehydrated with ethanol gradient, cleared with xylene and paraffin-

303   embedded. 3-µm thick eye sections were used for standard immunofluorescence

304   staining protocol. Images were acquired in a Leica DMR HC epifluorescence

305   microscope   (Leica   Microsystems).

306   Primary antibodies used were: Insulin (DAKO, 1:400), C-peptide (Abcam, 1: 200 or

307   Hybridoma Bank; 1:40), vimentin (Sigma, 1:200), HLA (Abcam, 1:100), Nkx-2.2

308   (Hybridoma Bank, 1:400), Pdx1 (Abcam 1:500) and MafA (Novus Biologicals 1:75).

309   The antigen-primary antibody immune complex was visualized with secondary

310   antibodies conjugated to Alexa Fluor 488 (Jackson Immunoresearch, 1:250), Alexa

311   fluor 555 (Molecular Probes, 1:400) or Alexa fluor 647 (Jackson Immunoreserach,

312   1:250). Cell nuclei were counterstained with Hoescht (SIGMA, 1:500). Representative

313   images were taken using a confocal microscope (LEICA TCS SPE).

314

315   **Statistical analysis**

316   Data are presented as mean ± standard error of the mean (SEM) from at least three

317   independent reprogramming experiments, with one to four biological replicates per

318   experiment. Significant differences between the means were analyzed by the two-tailed

319   unpaired Student's *t*-test, one sample t-test or one-way ANOVA followed by Tukey's

320   multiple comparison tests as indicated in the figure legends. Statistical analysis was

321   performed with GraphPad Prism 8.00 and Microsoft Office Excel 2007 and differences

322   were considered significant at p<0.05. No methods were used to determine whether

323   the data met assumptions of the statistical approach (e.g. test for normal distribution).

324

325   **RESULTS**

326   **Introduction of the transcription factors Pdx1, Ngn3 and MafA (PNM) leads to**

327   **activation of β-cell genes and insulin production by human fibroblasts.**

328   We first investigated whether human fibroblasts could be directly converted towards the

329   β-cell lineage through exogenous expression of the PNM factors Pdx1, Neurog3 and

330   MafA. As delivery method we used a polycistronic adenoviral vector encoding the three

331   transcription factors and a Cherry reporter protein (Ad-PNM hereafter) that had been

332   previously used in the reprogramming of pancreatic acinar cells towards islet cells [35].

333   We chose adenoviruses for transgene delivery because they allow high expression of

334   transgenic proteins and, most importantly, don't integrate in the host genome.

335   However, we couldn't detect Cherry immunofluorescence after viral treatment of human

336   fibroblasts (Fig. S1), which was in agreement with other reports showing poor

337   adenoviral transduction efficiency in fibroblastic cells [36, 37]. In an attempt to boost

338   adenoviral transduction, we added an activated dendrimer normally used in

339   transfections to the virus-containing media and, in stark contrast to Ad-PNM alone, we

340   observed abundant (>80%) fibroblasts that were Cherry[+] three days after exposure to

341   the virus+dendrimer (Fig.S1 and Fig.1A). Interestingly, Cherry^{+} cells were still readily

342   visible 7 days post-viral treatment (Fig. 1A). Likewise, transcripts encoding the PNM

343   factors were detected at 3 and 7 days after viral treatment (Fig.1B). Remarkably, three

344   days after addition of Ad-PNM we detected low levels of *INS* transcripts that were

345   dramatically increased by day 7 (Fig.1C). We examined the influence of distinct culture

346   media on *INS* mRNA levels and found that cells cultured in RPMI-1640 supplemented

13

347   with 6% FBS exhibited the highest degree of *INS* gene activation relative to cells

348   cultured in DMEM or CMRL-1066, reaching values that were 900-fold lower than

349   human islets but similar to those attained in directed differentiation protocols from iPSC

350   [38] (Fig. 1D). The PNM factors also induced moderate levels of several endocrine

351   transcription factor genes including *NEUROD1, INSM1, PAX4, NKX2-2* and *ARX*,

352   although they did not induce the key β-cell TF *NKX6-1* (Fig.1E). Unexpectedly, the

353   PNM factors also induced the islet hormone genes *GLUCAGON (GCG)* and

354   *SOMATOSTATIN (SST)*, albeit to levels less than those observed for *INS (*as indicated

355   by lower expression relative to the housekeeping gene *TATA BINDING PROTEIN,*

356   (*TBP*) (Fig. 1F). Conversely, PNM down-regulated the expression of genes associated

357   with fibroblast signature, including several factors involved in maintenance of the

358   fibroblastic transcriptional program such as *TWIST2*, *PRRX1* and *LHX9* [39] (Fig. 1G).

359   Together, these experiments show that the PNM factors induce a transcriptional switch

360   from a fibroblastic towards an endocrine program in human fibroblasts.

361   **Addition of Pax4 and Nkx2-2 to the PNM factors improves reprogramming of**

362   **human fibroblasts towards the β-cell lineage.**

363   Due to the suboptimal conversion of fibroblasts into β-like cells using the PNM factors

364   (i.e. as reflected by the lack of induction of *NKX6-1* mRNA and the expression of other

365   endocrine hormones), we tested the effects of adding other transcription factors to the

366   reprogramming cocktail, namely Nkx6-1, Pax4, NeuroD1 and Nkx2-2. Among all tested

367   combinations, we found that expression of PNM in a single polycistronic adenovirus

368   followed by sequential expression of Pax4 and Nkx2-2 (hereafter this combination is

369   named 5TF) resulted, ten days after initial PNM infection, in the highest degree of *INS*

370   gene activation accompanied by the blockade of *GCG* gene induction (Fig. 2A&B and

371   Fig.S2). Moreover, 5TF reprogramming resulted in activation of *NKX6.1* and of the

372   pan-endocrine factor *PAX6 genes (*Fig. 2B*).* At day 10, reprogrammed cells displayed

373   an epithelial morphology (Fig. 2C) and hadn't grown as much as untreated fibroblasts

374   (day 10; 5TF: $44 \times 10^3 \pm 3 \times 10^3$ cells/well; control: $238 \times 10^3 \pm 18 \times 10^3$ cells/well, n=18). In

375   fact, reprogrammed cells showed diminished proliferation as early as one day after

376   PNM introduction, while remaining viable, as indicated by their retained ability to

377   reduce MTT, similar to that of fibroblasts (Fig. 2D&E). At day 10, reprogrammed cells

378   exhibited lower MTT reduction activity, likely due to their decreased cell numbers (Fig.

379   2E).

380   Consistent with the gene expression data, insulin protein was detected by

381   immunofluorescence staining in both PNM and 5TF cells, being staining more robust in

382   5TF cells than in PNM cells (Fig. 2F). By contrast, neither glucagon nor somatostatin

383   proteins were detected in either PNM or 5TF cells. We quantified the

384   immunofluorescence images and found that $67.9 \pm 6.2\%$ of cells in the culture were

385   INS+ at day 10. The presence of endogenous insulin production was further confirmed

386   by immunofluorescence staining using an antibody against C-peptide (Fig.2G) and by

387   determining C-peptide content with an ELISA (control: 0.34 ± 0.14 pg/10^5 cells, n=9;

388   5TF: 16.06 ± 2.55 pg/10^5 cells, n=16). To further establish the extent of reprogramming

389   achieved with 5TF as compared to PNM, we studied expression of additional endocrine

390   genes at day 10. We found that transcripts of β-cell differentiation TFs (i.e. *NEUROD1*,

391   *INSM1*, *HNF1B, MAFB*), as well as some of the reprogramming TFs (*PDX1*,

392   *NEUROG3*, *NKX2-2*) were higher in 5TF as compared to PNM (Fig. 3A). On the other

393   hand, several genes associated with a mature β-cell phenotype were more upregulated

394   by 5TF than PNM (*PCSK1*, *ABCC8*, *KCNJ11, GLP1R, GIPR, NCAM1, CXCR4*), whilst

395   others (*CHGB*, *PTPRN*, *CX36*) were induced to similar extents by both TF

396   combinations (Fig. 3B). In line with loss of *GCG* activation, the pro-convertase gene

397   *PCSK2*, which is expressed at higher levels in α than β cells [40], was reduced by 5TF as

398   compared to PNM (Fig.3B), supporting that sequential introduction of Pax4 and Nkx2-2

399   after PNM endorses the β-cell differentiation program in human fibroblasts. It should be

400   noted that expression levels of the induced genes were lower than in human islets, with

15

401 differences ranging from 2-fold for *NCAM1* to 20,000-fold for *CHGB* (Fig. 3A,B, Table

402 S1). Gene activation was sustained for at least eleven additional days under the same

403 culture conditions despite declined expression of the reprogramming factor transgenes.

404 Moreover, expression of some genes increased with time in culture (i.e. *NKX6.1,*

405 *INSM1, ABCC8, CHGB*) (Fig.S3).

406 Lastly, we looked into genes that are selectively repressed (disallowed) in β cells [41]. In

407 response to 5TF, several β-cell disallowed genes were significantly downregulated

408 reaching expression levels comparable to human islets (*OAT*, *SMAD3*, *PDGFRA*,

409 *CXCL12*, *LDHA*), while others remained unchanged (*REST*, I*GFBP4*). Among the

410 studied genes only *MCT1* was induced by 5FT relative to parental HFF1 cells (Fig.3C).

411 Together, these results reveal that 5TF induces a transcriptional switch from a

412 fibroblastic to a β-like cell identity that entails both selective gene activation and

413 repression events. Hereafter, we will refer to cells generated following the 5TF protocol

414 as induced β-like (iβ-like) cells.

415 **In vitro assessment of human fibroblast-derived iβ-like cells.**

416 Glucose-induced insulin secretion (GSIS) by β cells is mediated by glucose

417 metabolism, closure of ATP-dependent potassium channels, membrane depolarization

418 and opening of voltage-dependent calcium channels, resulting in an increase in

419 cytosolic Ca^{2+} that triggers insulin exocytosis. We investigated whether iβ-like cells

420 exhibited β-cell functional features *in vitro* and begun by determining their ability to

421 increase intracellular Ca^{2+} in response to glucose and membrane depolarization elicited

422 by high potassium. We found that 65% of the cells exhibited a response to glucose,

423 high potassium, or both whilst 35% of cells were unresponsive to either stimulus (Fig.

424 4A and video S1). Parental HFF1 cells not engineered for 5TF expression were

425 universally unresponsive to these stimuli (Fig. 4B and video S2). Among responsive

426 cells, approximately half responded to both glucose and high potassium and half

427 responded only to potassium (Fig. 4A). We observed heterogeneity in the amplitude

428 and kinetics of responses among individual cells (Fig. 4C). Next, we performed static

429 incubation assays to study glucose-induced insulin secretion (GSIS) and found that iβ-

430 like cells released similar amounts of human insulin at low (2mM) and high (20mM)

431 glucose concentrations (Fig.4D). Thus, at this stage, iβ-like cells lack a key signature

432 feature of normal β-cells, the ability to increase insulin secretion in response to

433 changes in extracellular glucose.

434 The differentiation and functionality of many cell types vary dramatically between three-

435 dimensional (3D) and two-dimensional (2D) monolayer cultures, the former being

436 closer to the natural 3D microenvironment of cells in a living organism. Considering

437 this, we reasoned that moving from the planar cell culture to a 3D system grown in

438 suspension might improve the functionality of iβ-like cells. To test this, we generated

439 spheroids of 1 200-1 800 iβ-like cells (average diameter of spheroids were 128±27 μm)

440 one day after introduction of Nkx2-2 and maintained them in culture for three additional

441 days (Fig.5A). Insulin protein was readily detected by immunostaining (Fig. 5B).

442 Further, iβ-like cell spheroids presented higher transcript levels for several β-cell

443 maturation markers including *INS*, the prohormone convertase *PCSK1*, and the ATP-

444 dependent potassium channel subunits *KCNJ11* and *ABCC8*, as compared to iβ-like

445 cells maintained in 2D cultures (Fig.5C). Consequently, the differences in expression

446 levels with human islets were reduced (Table S2). Consistent with improved

447 maturation; iβ-like cell spheroids exhibited a moderate but significant insulin secretory

448 response to glucose (fold 20mM/2mM: 2.02±0.18) as compared to 2D cultures (fold

449 20mM/2mM: 1.08-±0.15) in static GSIS assays (Fig. 5D,E). Similar results were

450 obtained using a different preparation of human foreskin fibroblasts (Fig. S4).

451 Therefore, three-dimensional culture during the last stage of the 5TF reprogramming

452 protocol (note that total length of the protocol remained unchanged) improved iβ-like

453 cell function

454

455   To establish the glucose threshold for stimulation of insulin secretion, iβ-like cell

456   clusters were subjected to either 2,5,11 or 20mM glucose. Although there was some

457   variability, when moved from 2mM to 5mM glucose, cells did not show a statistical

458   significant increase in insulin secretion (Fig. 5F). They increased insulin secretion on

459   average by a factor of 2.3 when moved from 2mM to 11mM or to 20mM glucose (Fig.

460   5F). These observations indicate that iβ-like cells are stimulated at higher glucose

461   threshold. Remarkably, this concentration dependence of insulin secretion is similar to

462   human islets that have a threshold at 3mM and a maximal response at 15mM [39]. In

463   light of these results, we asked whether iβ-like cells presented recognizable secretory

464   granules. Therefore, iβ-like cell clusters where fixed and prepared for conventional

465   electron microscopy. The presence of multiple spherical electron-dense prototypical

466   secretory vesicles was evident in most cells (Fig. 5G). These vesicles showed a high

467   degree of morphological heterogeneity, presumably as consequence of their degree of

468   maturation and/or loading. Although they did not have the appearance of typical

469   insulin-containing granules from primary β cells, which are characterized by a clear

470   halo surrounding a dark polygonal dense core [42], some of the vesicles exhibited a grey

471   or less electron dense halo and looked similar to the granules described in insulin-

472   positive cells generated from stem cells in original differentiation protocols [10, 43].

473

474   **In vivo assessment of human fibroblast-derived iβ-like cells.**

475   Lastly, we studied the maintenance of cellular reprogramming in vivo. To this end, we

476   transplanted 300 iβ-like cell spheroids (1000 cells/spheroid) into the anterior chamber

477   of the eye (ACE) of immune-deficient NOD *scid* gamma (NSG) mice (Fig. 6A,B). The

478   ACE allows fast engraftment [44] and *in vivo* imaging[45]. To assess *in vivo* graft

479   revascularization we used two-photon microscopy after injection of RITC-dextran and

480   confirmed the presence of functional vessels in the grafts 10 days after transplantation

18

481   (Fig. 6C and video S1). We also established that the transplanted cells were viable by

482   visualizing fluorescence of the long-term tracer CFDA (Fig. 6C). We then investigated

483   whether reprogramming was retained in vivo. We first studied human *INS* gene

484   expression in eye grafts harvested ten days after transplantation. As shown in Figure

485   6D, human *INS* transcripts were readily detectable and levels (expressed relative to

486   *TBP*) were similar to those exhibited by iβ-like cells prior to transplantation (Fig.2A, Fig.

487   5C). Corroborating this result, there were abundant HLA+ (human cell marker) cells

488   that stained for C-peptide and for the transcription factors PDX1, NKX2-2 and MAFA,

489   which are produced from both viral transgenes and cellular genes, in the eye grafts

490   (Fig. 6E and Fig. S5). Of the total number of HLA+ cells counted, 43.5±2.7% were also

491   positive for C-peptide (Fig. 6F). In addition, thirty minutes after an intra-peritoneal

492   glucose injection, human insulin was readily detectable in the aqueous humor of the

493   eyes carrying iβ-like cell grafts (17 of 17, ranging from 11 to 158 mU/L), whereas no

494   insulin was detected in eyes transplanted with non-engineered fibroblast clusters or in

495   mice that received no transplants (Fig.6G). Average insulin levels achieved with 300 iβ-

496   like cells were around 10-fold lower than those observed with 150-200 human islets

497   (53±11 mU/L as compared to 688±99mU/L) (Fig. 6G). Together, these data confirm

498   that cellular reprogramming persisted after transplantation.

499   Finally, to evaluate iβ-like cell function in vivo, approximately 4000 spheroids were

500   loaded onto a collagen disk and deposited subcutaneously into the abdominal cavity of

501   adult NSG mice. We detected low levels of circulating human insulin after a glucose

502   challenge in 3 (of 3) and 2 (of 3) mice at days 15 and 30 post-transplantation,

503   respectively (Fig. 6H). We repeated this experiment using the well-vascularized

504   omentum as implant site and observed overall higher human insulin levels and

505   significant glucose-stimulated insulin secretion at day 30 post-transplantation in 3 (of 3)

506   mice (Fig. 6H). Together, these results demonstrate that iβ-like cells exhibit glucose-

507   induced insulin secretion in vivo. Remarkably, glucose-induced plasma human insulin

508   levels observed in mice transplanted with 4000 iβ-like cell spheroids were in the same

509   order of magnitude than mice transplanted with a total of 300-500 human islets into the

510   ACE (Fig. 6H). Thus, correlating with determinations in the aqueous humor, these

511   results reveal that iβ-like cell clusters secrete *in vivo* approximately one tenth of the

512   amount of insulin released by human islets.

513   **DISCUSSION**

514   In this study, we have developed a 10-day long protocol to produce insulin-producing

515   cells from human fibroblasts through sequential introduction of five lineage-determining

516   transcription factors. Enforced expression of PNM+Pax4+Nkx2-2 results in concomitant

517   activation of the β-cell and down-regulation of the fibroblastic transcriptional programs.

518   Significantly, reprogrammed cells exhibit a functional β-cell like phenotype as judged by

519   their expression of critical β-cell function genes and their ability to mobilize calcium and

520   secrete insulin upon glucose stimulation. These findings warrant further investigations

521   on TF-based reprogramming strategies to generate β-like cells from human fibroblasts.

522   When compared to other published TF-based reprogramming examples, iβ-like cells

523   exhibited *INS* transcript levels similar to those of reprogrammed human pancreatic duct

524   cells [20] and remarkably higher than those reached in human hepatocytes [46]. Still,

525   expression levels of insulin and of other β-cell marker genes were lower than in human

526   islets. Likewise, glucose-induced insulin secretion was modest, especially in terms of

527   the amount of hormone secreted. We expect further progress by redefining culture

528   conditions as it has been done in stem cell derivation protocols for more than a decade

529   [7, 10, 43, 47-52]. For example here we report that, by merely moving from 2D to a 3D culture

530   system, iβ-like cells acquired the ability to secrete insulin in response to glucose.

531   Another simple strategy to improve the functionality of iβ-like cells would be the

532   addition of soluble factors during or after introduction of the conversion TFs [38, 53, 54].

533   Some of these factors might be selected from the growing body of information on

534   molecules that enhance maturation of β cells generated from stem cells [55].

535   Interestingly, it has been shown that soluble molecules can even substitute the function

536   of exogenous factors in some reprogramming protocols [56-58].

537   The use of skin fibroblasts as cell source in place of other less accessible cell lineages

538   can facilitate clinical translation of this approach. Furthermore, the prospect of auto-

539   transplantation and the avoidance of tumor-related concerns linked to pluripotent cell

540   states are two additional assets of this type of direct reprogramming approaches. Here

541   we show that iβ-like cell grafts are efficiently re-vascularized, viable and exhibit

542   glucose-induced insulin secretion in vivo. Circulating human insulin levels in mice

543   transplanted with iβ-like cells were lower but not far-off from those reported in

544   publications using stem cell-derived insulin-producing cells (Table S2). Together, these

545   results provide the foundation for further work aimed at evaluating the long-term

546   function of transplanted iβ-like cell spheroids under pathophysiological contexts. It will

547   be interesting to assess whether the in vivo environment aids in the maturation process

548   of iβ-like cells as it has been reported for stem cell-derived β cell progenitors [49, 52].

549   In summary, our results demonstrate that it is possible to generate insulin-producing

550   cells from human fibroblasts using lineage specific transcription factors. This work

551   evidences the feasibility of direct lineage reprogramming to generate β-like cells from

552   developmentally distant cell lineages. The relative technical simplicity and speed of this

553   procedure together with the opportunity to generate patient-specific β cells for disease

554   modeling and/or autologous transplantation warrants a more comprehensive evaluation

555   of this approach in the future.

556

557   **ACKNOWLEDGEMENTS**

21

581   **AUTHOR CONTRIBUTIONS**

582   Conceived and designed the experiments: MF, RGa. Performed the experiments: MF,

583   AG, EP, NT, HF, RFR, SC. Provided human islets: CB, AW. Provided materials: LC,

584   JR, NM, AN. Analyzed and discussed the data: MF, CE, JV, RGo, RGa. Wrote the

585   manuscript: MF, RGa.

586   **CONFLICT OF INTEREST**

587   Authors declare no conflict of interest

588   **REFERENCES**

589   1.   Takahashi K, Tanabe K, Ohnuki M, Narita M, Ichisaka T, Tomoda K*, et al.*
590   Induction of pluripotent stem cells from adult human fibroblasts by defined
591   factors. *Cell* 2007, **131**(5)**:** 861-872.
592

593   2.   Takahashi K, Yamanaka S. Induction of pluripotent stem cells from mouse
594   embryonic and adult fibroblast cultures by defined factors. *Cell* 2006, **126**(4)**:**
595   663-676.
596

597   3.   Graf T. Historical origins of transdifferentiation and reprogramming. *Cell stem*
598   *cell* 2011, **9**(6)**:** 504-516.
599

600   4.   Vierbuchen T, Wernig M. Molecular roadblocks for cellular reprogramming.
601   *Molecular cell* 2012, **47**(6)**:** 827-838.
602

603   5.   Xu J, Du Y, Deng H. Direct lineage reprogramming: strategies, mechanisms,
604   and applications. *Cell stem cell* 2015, **16**(2)**:** 119-134.
605

606   6.   Yamanaka S. A fresh look at iPS cells. *Cell* 2009, **137**(1)**:** 13-17.
607

608   7.   D'Amour KA, Agulnick AD, Eliazer S, Kelly OG, Kroon E, Baetge EE. Efficient
609   differentiation of human embryonic stem cells to definitive endoderm. *Nature*
610   *biotechnology* 2005, **23**(12)**:** 1534-1541.
611

612   8.   Kroon E, Martinson LA, Kadoya K, Bang AG, Kelly OG, Eliazer S*, et al.*
613   Pancreatic endoderm derived from human embryonic stem cells generates
614   glucose-responsive insulin-secreting cells in vivo. *Nature biotechnology* 2008,
615   **26**(4)**:** 443-452.
616

617   9.   Maehr R, Chen S, Snitow M, Ludwig T, Yagasaki L, Goland R*, et al.* Generation
618   of pluripotent stem cells from patients with type 1 diabetes. *Proceedings of the*
619   *National Academy of Sciences of the United States of America* 2009, **106**(37)**:**
620   15768-15773.
621

622   10.   Pagliuca FW, Millman JR, Gurtler M, Segel M, Van Dervort A, Ryu JH*, et al.*
623   Generation of functional human pancreatic beta cells in vitro. *Cell* 2014, **159**(2)**:**
624   428-439.
625

626   11.   Rezania A, Bruin JE, Arora P, Rubin A, Batushansky I, Asadi A*, et al.* Reversal
627   of diabetes with insulin-producing cells derived in vitro from human pluripotent
628   stem cells. *Nature biotechnology* 2014, **32**(11)**:** 1121-1133.
629

12. Johnson JD. The quest to make fully functional human pancreatic beta cells from embryonic stem cells: climbing a mountain in the clouds. *Diabetologia* 2016, **59**(10)**:** 2047-2057.

13. Kushner JA, MacDonald PE, Atkinson MA. Stem cells to insulin secreting cells: two steps forward and now a time to pause? *Cell stem cell* 2014, **15**(5)**:** 535-536.

14. Zhou Q, Brown J, Kanarek A, Rajagopal J, Melton DA. In vivo reprogramming of adult pancreatic exocrine cells to beta-cells. *Nature* 2008, **455**(7213)**:** 627-632.

15. Ariyachet C, Tovaglieri A, Xiang G, Lu J, Shah MS, Richmond CA*, et al.* Reprogrammed Stomach Tissue as a Renewable Source of Functional beta Cells for Blood Glucose Regulation. *Cell stem cell* 2016, **18**(3)**:** 410-421.

16. Chen YJ, Finkbeiner SR, Weinblatt D, Emmett MJ, Tameire F, Yousefi M*, et al.* De novo formation of insulin-producing "neo-beta cell islets" from intestinal crypts. *Cell reports* 2014, **6**(6)**:** 1046-1058.

17. Furuyama K, Chera S, van Gurp L, Oropeza D, Ghila L, Damond N*, et al.* Diabetes relief in mice by glucose-sensing insulin-secreting human alpha-cells. *Nature* 2019.

18. Gasa R, Mrejen C, Leachman N, Otten M, Barnes M, Wang J*, et al.* Proendocrine genes coordinate the pancreatic islet differentiation program in vitro. *Proceedings of the National Academy of Sciences of the United States of America* 2004, **101**(36)**:** 13245-13250.

19. Heremans Y, Van De Casteele M, in't Veld P, Gradwohl G, Serup P, Madsen O*, et al.* Recapitulation of embryonic neuroendocrine differentiation in adult human pancreatic duct cells expressing neurogenin 3. *The Journal of cell biology* 2002, **159**(2)**:** 303-312.

20. Lee J, Sugiyama T, Liu Y, Wang J, Gu X, Lei J*, et al.* Expansion and conversion of human pancreatic ductal cells into insulin-secreting endocrine cells. *eLife* 2013, **2:** e00940.

21. Yechoor V, Liu V, Espiritu C, Paul A, Oka K, Kojima H*, et al.* Neurogenin3 is sufficient for transdetermination of hepatic progenitor cells into neo-islets in vivo but not transdifferentiation of hepatocytes. *Developmental cell* 2009, **16**(3)**:** 358-373.

22. Ieda M, Fu JD, Delgado-Olguin P, Vedantham V, Hayashi Y, Bruneau BG*, et al.* Direct reprogramming of fibroblasts into functional cardiomyocytes by defined factors. *Cell* 2010, **142**(3)**:** 375-386.

23. Hiramatsu K, Sasagawa S, Outani H, Nakagawa K, Yoshikawa H, Tsumaki N. Generation of hyaline cartilaginous tissue from mouse adult dermal fibroblast culture by defined factors. *The Journal of clinical investigation* 2011, **121**(2)**:** 640-657.

24. Vierbuchen T, Ostermeier A, Pang ZP, Kokubu Y, Sudhof TC, Wernig M. Direct conversion of fibroblasts to functional neurons by defined factors. *Nature* 2010, **463**(7284)**:** 1035-1041.

685

686 25. Najm FJ, Lager AM, Zaremba A, Wyatt K, Caprariello AV, Factor DC*, et al.*
687   Transcription factor-mediated reprogramming of fibroblasts to expandable,
688   myelinogenic oligodendrocyte progenitor cells. *Nature biotechnology* 2013,
689   **31**(5)**:** 426-433.
690

691 26. Zhu S, Russ HA, Wang X, Zhang M, Ma T, Xu T*, et al.* Human pancreatic beta-
692   like cells converted from fibroblasts. *Nature communications* 2016, **7:** 10080.
693

694 27. Pennarossa G, Maffei S, Campagnol M, Tarantini L, Gandolfi F, Brevini TA.
695   Brief demethylation step allows the conversion of adult human skin fibroblasts
696   into insulin-secreting cells. *Proceedings of the National Academy of Sciences of*
697   *the United States of America* 2013, **110**(22)**:** 8948-8953.
698

699 28. Pereyra-Bonnet F, Gimeno ML, Argumedo NR, Ielpi M, Cardozo JA, Gimenez
700   CA*, et al.* Skin fibroblasts from patients with type 1 diabetes (T1D) can be
701   chemically transdifferentiated into insulin-expressing clusters: a transgene-free
702   approach. *PloS one* 2014, **9**(6)**:** e100369.
703

704 29. Akinci E, Banga A, Tungatt K, Segal J, Eberhard D, Dutton JR*, et al.*
705   Reprogramming of various cell types to a beta-like state by Pdx1, Ngn3 and
706   MafA. *PloS one* 2013, **8**(11)**:** e82424.
707

708 30. Katz LS, Geras-Raaka E, Gershengorn MC. Reprogramming adult human
709   dermal fibroblasts to islet-like cells by epigenetic modification coupled to
710   transcription factor modulation. *Stem cells and development* 2013, **22**(18)**:**
711   2551-2560.
712

713 31. Broca C, Varin E, Armanet M, Tourrel-Cuzin C, Bosco D, Dalle S*, et al.*
714   Proteasome dysfunction mediates high glucose-induced apoptosis in rodent
715   beta cells and human islets. *PloS one* 2014, **9**(3)**:** e92066.
716

717 32. Lynn FC, Sanchez L, Gomis R, German MS, Gasa R. Identification of the bHLH
718   factor Math6 as a novel component of the embryonic pancreas transcriptional
719   network. *PloS one* 2008, **3**(6)**:** e2430.
720

721 33. Bartholomeus K, Jacobs-Tulleneers-Thevissen D, Shouyue S, Suenens K, In't
722   Veld PA, Pipeleers-Marichal M*, et al.* Omentum is better site than kidney
723   capsule for growth, differentiation, and vascularization of immature porcine
724   beta-cell implants in immunodeficient rats. *Transplantation* 2013, **96**(12)**:** 1026-
725   1033.
726

727 34. Figueiredo H, Figueroa ALC, Garcia A, Fernandez-Ruiz R, Broca C,
728   Wojtusciszyn A*, et al.* Targeting pancreatic islet PTP1B improves islet graft
729   revascularization and transplant outcomes. *Science translational medicine*
730   2019, **11**(497).
731

732 35. Li W, Nakanishi M, Zumsteg A, Shear M, Wright C, Melton DA*, et al.* In vivo
733   reprogramming of pancreatic acinar cells to three islet endocrine subtypes.
734   *eLife* 2014, **3:** e01846.
735

736 36. Granio O, Porcherot M, Corjon S, Kitidee K, Henning P, Eljaafari A*, et al.*
737   Improved adenovirus type 5 vector-mediated transduction of resistant cells by
738   piggybacking on coxsackie B-adenovirus receptor-pseudotyped baculovirus.
739   *Journal of virology* 2009, **83**(12)**:** 6048-6066.

37. Toh ML, Hong SS, van de Loo F, Franqueville L, Lindholm L, van den Berg W, *et al.* Enhancement of adenovirus-mediated gene delivery to rheumatoid arthritis synoviocytes and synovium by fiber modifications: role of arginine-glycine-aspartic acid (RGD)- and non-RGD-binding integrins. *Journal of immunology* 2005, **175**(11): 7687-7698.

38. Fontcuberta-PiSunyer M, Cervantes S, Miquel E, Mora-Castilla S, Laurent LC, Raya A, *et al.* Modulation of the endocrine transcriptional program by targeting histone modifiers of the H3K27me3 mark. *Biochimica et biophysica acta* 2018, **1861**(5): 473-480.

39. Tomaru Y, Hasegawa R, Suzuki T, Sato T, Kubosaki A, Suzuki M, *et al.* A transient disruption of fibroblastic transcriptional regulatory network facilitates trans-differentiation. *Nucleic acids research* 2014, **42**(14): 8905-8913.

40. Ramzy AK, T.J. Revisiting Proinsulin Processing: Evidence That Human β-Cells Process Proinsulin With Prohormone Convertase (PC) 1/3 but Not PC2. *Diabetes* 2020, **69:** 1451-1462.

41. Schuit FVL, J; Granvik,M; Goyvaerts, L; de Faudeur, Gd, Schraenen, A; Lemaire, K. b-Cell–Specific Gene Repression: A Mechanism to Protect Against Inappropriate or Maladjusted Insulin Secretion? *Diabetes* 2012, **61:** 969-975.

42. Brereton MF, Vergari E, Zhang Q, Clark A. Alpha-, Delta- and PP-cells: Are They the Architectural Cornerstones of Islet Structure and Co-ordination? . *J Histochem Cytochem* 2015, **63:** 575-591.

43. D'Amour KA, Bang AG, Eliazer S, Kelly OG, Agulnick AD, Smart NG, *et al.* Production of pancreatic hormone-expressing endocrine cells from human embryonic stem cells. *Nature biotechnology* 2006, **24**(11): 1392-1401.

44. Adeghate E, Donath T. Morphological findings in long-term pancreatic tissue transplants in the anterior eye chamber of rats. *Pancreas* 1990, **5**(3): 298-305.

45. Leibiger IB, Berggren PO. Intraocular in vivo imaging of pancreatic islet cell physiology/pathology. *Molecular metabolism* 2017, **6**(9): 1002-1009.

46. Sapir T, Shternhall K, Meivar-Levy I, Blumenfeld T, Cohen H, Skutelsky E, *et al.* Cell-replacement therapy for diabetes: Generating functional insulin-producing tissue from adult human liver cells. *Proceedings of the National Academy of Sciences of the United States of America* 2005, **102**(22): 7964-7969.

47. Russ HA, Parent AV, Ringler JJ, Hennings TG, Nair GG, Shveygert M, *et al.* Controlled induction of human pancreatic progenitors produces functional beta-like cells in vitro. *The EMBO journal* 2015, **34**(13): 1759-1772.

48. Rezania A, Bruin JE, Xu J, Narayan K, Fox JK, O'Neil JJ, *et al.* Enrichment of human embryonic stem cell-derived NKX6.1-expressing pancreatic progenitor cells accelerates the maturation of insulin-secreting cells in vivo. *Stem cells* 2013, **31**(11): 2432-2442.

49. Rezania A, Bruin JE, Riedel MJ, Mojibian M, Asadi A, Xu J, *et al.* Maturation of human embryonic stem cell-derived pancreatic progenitors into functional islets

capable of treating pre-existing diabetes in mice. *Diabetes* 2012, **61**(8)**:** 2016-2029.

50. Liu H, Li R, Liao H-K, Min Z, Wang C, Yu Y*, et al.* Chemical combinations potentiate human pluripotent stem cell-derived 3D pancreatic progenitor clusters toward functional β cell. *Nature communications* 2021, **12:** 3330.

51. Hrvatin S, O'Donnell CW, Deng F, Millman JR, Pagliuca FW, DiIorio P*, et al.* Differentiated human stem cells resemble fetal, not adult, beta cells. *Proceedings of the National Academy of Sciences of the United States of America* 2014, **111**(8)**:** 3038-3043.

52. Bruin JE, Rezania A, Xu J, Narayan K, Fox JK, O'Neil JJ*, et al.* Maturation and function of human embryonic stem cell-derived pancreatic progenitors in macroencapsulation devices following transplant into mice. *Diabetologia* 2013, **56**(9)**:** 1987-1998.

53. Liu ML, Zang T, Zou Y, Chang JC, Gibson JR, Huber KM*, et al.* Small molecules enable neurogenin 2 to efficiently convert human fibroblasts into cholinergic neurons. *Nature communications* 2013, **4:** 2183.

54. Zhu S, Li W, Zhou H, Wei W, Ambasudhan R, Lin T*, et al.* Reprogramming of human primary somatic cells by OCT4 and chemical compounds. *Cell stem cell* 2010, **7**(6)**:** 651-655.

55. Ma X, Zhu S. **Chemical strategies for pancreatic β cell differentiation, reprogramming, and regeneration**. *Acta Biochim Biophys Sin (Shanghai)* 2017, **49:** 289-301.

56. Hu W, Qiu B, Guan W, Wang Q, Wang M, Li W*, et al.* Direct Conversion of Normal and Alzheimer's Disease Human Fibroblasts into Neuronal Cells by Small Molecules. *Cell stem cell* 2015, **17**(2)**:** 204-212.

57. Li K, Zhu S, Russ HA, Xu S, Xu T, Zhang Y*, et al.* Small molecules facilitate the reprogramming of mouse fibroblasts into pancreatic lineages. *Cell stem cell* 2014, **14**(2)**:** 228-236.

58. Fu Y, Huang C, Xu X, Gu H, Ye Y, Jiang C*, et al.* Direct reprogramming of mouse fibroblasts into cardiomyocytes with chemical cocktails. *Cell research* 2015, **25**(9)**:** 1013-1024.

FIGURE LEGENDS

Figure 1. Introduction of the PNM factors in human fibroblasts.

Human foreskin fibroblasts (HFF1) were transduced with a polycistronic recombinant adenovirus encoding the transcription factors Pdx1, Neurog3, MafA and the reporter

27

841   protein Cherry (Ad-PNM). Untreated parental fibroblasts were used as controls

842   (indicated as C in graphs). **(A)** Bright field images and Cherry immunofluorescence of

843   control fibroblasts and fibroblasts infected with Ad-PNM at day 3 and 7 post-infection.

844   Scale bar is 100 μm. **(B)** qRT-PCR of adenovirus-encoded transgenes at day 3 (n=11)

845   and 7 (n=6) after infection with Ad-PNM**. (C)** qRT-PCR of human *INS* at day 3 (n=7)

846   and 7 (n=13) after infection with Ad-PNM. **(D)** In red, qRT-PCR of human *INS* in

847   fibroblasts maintained in the indicated culture media during 7 days after infection with

848   the indicated adenoviruses, (n=3-10). In blue, *INS* mRNA levels in iPSC-derived β-cells

849   and in isolated human islets (n=10). **(E-F)** qRT-PCR of indicated genes encoding

850   islet/β-cell transcription factors and islet hormones at day 7 post-PNM (n=8-15). **(G)**

851   qRT-PCR for the indicated fibroblast markers at days 3 (n=5-11) and 7 post-PNM (n=5-

852   6). In **B-F**, expression levels are expressed relative to *TBP.* In *G*, expression is relative

853   to control fibroblasts, given the value of 1 (dotted line). Data are presented as the mean

854   ± SEM for the number of samples indicated in parenthesis. *,P<0.05; **,P<0.01;

855   ***,P<0.001, relative to control (untreated) fibroblasts or between indicated conditions

856   using unpaired t-test (**B-E**) or one sample t-test (**G**).

857

858   **Figure 2. Sequential introduction of the PNM factors, Pax4 and Nkx2-2 (5 TF**

859   **protocol) in human fibroblasts.**

860   **(A)** qRT-PCR for the indicated genes in HFF1 fibroblasts infected with different

861   combinations of the indicated adenoviruses. Pax4 was added three days after PNM.

862   Nkx2-2 was added three days (PNM+Nkx2-2) or six days (PNM+Pax4+Nkx2-2) after

863   PNM. Expression levels are calculated relative to *TBP* (n=4-12). **(B)** Scheme of the

864   final 5TF reprogramming protocol showing the sequence of addition of adenoviruses

865   encoding the indicated transcription factor/s. Duration of incubation with each

866   adenovirus is represented with a line. Cells were studied at days 9-10 after initial

867   addition of Ad-PNM. **(C)** Representative bright field image of parental fibroblasts and

868   5TF reprogrammed fibroblasts at day 10. **(D)** Cell proliferation measured by BrdU

869   incorporation (n=3) and **(E)** Cell viability measured by MTT assay (n=3) in untreated

870   control (in black) and 5TF-reprogrammed fibroblasts (in red) at the indicated days. Day

871   4 values are before Pax4 introduction. **(F-G)** Representative immunofluorescence

872   images showing Insulin and C-peptide staining (in red) in untreated fibroblasts and in

873   fibroblasts infected with Ad-PNM alone or with 5TF. Nuclei were stained with Hoechst

874   (in blue). Scale bar is 25 µm. Data are presented as the mean ± SEM for the number of

875   experiments indicated in parenthesis *,P<0.05; **,P<0.01; ***,P<0.001, P<0.0001

876   relative to PNM (in **A**) or to control fibroblasts (**D,E**) using one-way ANOVA (**A**), one-

877   sample t-test (**D**) or unpaired t-test (**E**).

878

879   **Figure 3. 5FT protocol promotes β-cell specific gene activation and repression**

880   **events in human fibroblasts.**

881   **(A,B)** qRT-PCR of islet/β-cell transcription factor **(A)** and β-cell function **(B)** genes in

882   untreated control fibroblasts (n=5-19), in fibroblasts infected with Ad-PNM alone (n=3-

883   20) or with 5TF (n=5-18) and in human islets (n=6-9). **(C)** qRT-PCR of β-cell

884   disallowed genes in untreated control fibroblasts (n=5), in fibroblasts infected with 5TF

885   (n=5-8) and in human islets (n=5). Expression levels were calculated relative to *TBP*.

886   Values represent the mean ± SEM for 5-14 for the number of n indicated in parenthesis

887   *, P< 0.05, **, P< 0.01, ***, P< 0.001 between indicated bars using unpaired t-test.

888

889   **Figure 4. Functional characterization of iβ-like cells generated with the 5TF**

890   **protocol.**

891   iβ-like cells were loaded with the calcium indicator Fluo-4-AM at day 10 of the 5TF

892   protocol. Single-cell imaging to detect cytosolic calcium was performed in the following

893   sequence: low glucose (2mM, G2), high glucose (20mM, G20) and membrane

894   depolarization with KCl 30mM. **(A)** Quantification of the frequency of cells (n=200, from

895   6 independent reprogramming experiments) that responded to glucose, membrane

896   depolarization elicited by high potassium or both. Representative measurements of

897   dynamic Fluo-4 fluorescence for **(B)** six single fibroblasts and **(C)** four single iβ-like

898   cells. **(D)** In vitro insulin secretion by iβ-like cells. ELISA determination of secreted

899   human insulin by control fibroblasts and iβ-like cells under non-stimulatory conditions

900   (glucose 2mM) and stimulatory conditions (glucose 20 mM). Data are mean ± SEM for

901   6 independent reprogramming experiments.

902

903   **Figure 5. In vitro characterization of iβ-like cell spheroids.**

904   **(A)** Schematic representation of the modified 5TF protocol: cells were moved from 2D

905   to 3D culture during the last three days (days 7-10) of the protocol. Bright field image of

906   generated iβ-like cell spheroids. Scale bar is 100 μm. **(B)** Representative

907   immunofluorescence image showing C-peptide staining in red and nuclei in blue

908   (marked with Hoechst) of an iβ-like cell spheroid at the end of the reprogramming

909   protocol. Scale bar is 100 μm. **(C)** qRT-PCR of the indicated genes in iβ-like cell

910   spheroids (n=9-16). Transcript levels are expressed as fold relative to levels in iβ-like

911   cells maintained in 2D culture throughout the 10-day protocol (given the value of 1,

912   dotted line). **(D)** In vitro glucose-induced insulin secretion by iβ-like cell spheroids

913   (n=14, from 8 reprogramming experiments). Secretion by control spheroids composed

914   of parental fibroblasts (n= 5) is also shown. **(E)** Glucose secretory Index (fold-response

915   20mM vs. 2mM glucose) of iβ-like cells maintained in 2D or in 3D (spheroids) cultures

916   (n=16-18, from 8-10 reprogramming experiments). **(F)** Glucose dose curve of insulin

917   secretion by iβ-like cell spheroids (n=4-12, 5 reprogramming experiments). **(G)**

918   Conventional transmission electron microscopy showing a representative image of iβ-

919   like cell spheroids. Prototypical electron dense secretory vesicles (asterisks) are

920   observed dispersed in the cytoplasm. Well-preserved mitochondria (mit), endoplasmic

921   reticulum (ER), Golgi membranes (G) and lipid droplets (LD) are also observed. Inset

922   shows a detail of a secretory vesicle with an average diameter of 450nm. N, nucleus.

923   Scale bars are 200nm (inset) and 500nm. Data are presented as the mean ± SEM for

924   the number of experiments (n) indicated in parenthesis. *,P<0.05; **,P<0.01;

925   ***,P<0.001, relative to 2D iβ cells **(C,E)**, or between glucose concentrations **(D,F)**

926   using one sample t-test **(C)**, unpaired t test **(D, E)** or one-way ANOVA **(F)**.

927

928   **Figure 6. In vivo characterization of iβ-like cell spheroids.**

929   **(A)** Schematic representation of the transplantation of iβ-like cell spheroids into the

930   anterior chamber of the eye (ACE) of immunodeficient NSG mice. **(B)** Image of an eye

931   recently transplanted with 300 iβ-like cell spheroids (1000 cells/spheroid). **(C)**

932   Vascularization of iβ-like cell aggregate grafts ten days following transplantation into

933   the ACE. Representative in vivo image of functional vessels (RITC-dextran, red) and

934   viable iβ-like cells (CFDA, green). Scale bar is 100 μm. **(D)** qRT-PCR of human *TBP*

935   and human INS transcripts in eyes of non-transplanted mice (n=3) and mice

936   transplanted with fibroblast spheroids (n=3) or iβ-like cell spheroids (n=5) collected ten

937   days post-transplantation. Human *TBP* expression is calculated relative to mouse *Tbp*

938   and human *INS* relative to human *TBP*. **(E)** Representative immunofluorescence

939   images showing HLA staining in red and C-peptide staining in green in iβ-like cell

940   spheroid grafts ten days post-transplantation in NSG mice. Scale bar is 25 μm. **(F)**

941   Percentage of C-peptide+/HLA+ in eye grafts ten days after transplantation (n=5). **(G)**

942   ELISA determination of human insulin in the aqueous humor after a glucose bolus in

943   un-transplanted mice (n=7), in control mice transplanted with fibroblast spheroids

944   (n=16) and in mice transplanted with iβ-like cell spheroids (n= 17) in the ACE at day 10

945   post-transplantation; and in mice transplanted with 150-200 human islets (n=3) in the

946   ACE at day 12-15 post-transplantation. **(H)** ELISA determination of human insulin in

947   plasma, before and after a glucose challenge, at days 15 and 30 after transplantation

948   of iβ-like cell spheroids subcutaneously (n=3) or in the omentum (n=3) of NSG mice.

949   Each individual mouse is represented by a different color. Plasma human insulin levels

950   in non-transplanted animals (n=3), before and after glucose administration, and in

951   animals transplanted with human islets in the ACE (n=5), after a glucose bolus, are

952   provided for comparison purposes. Data are presented as mean ± SEM. ***, P< 0.001
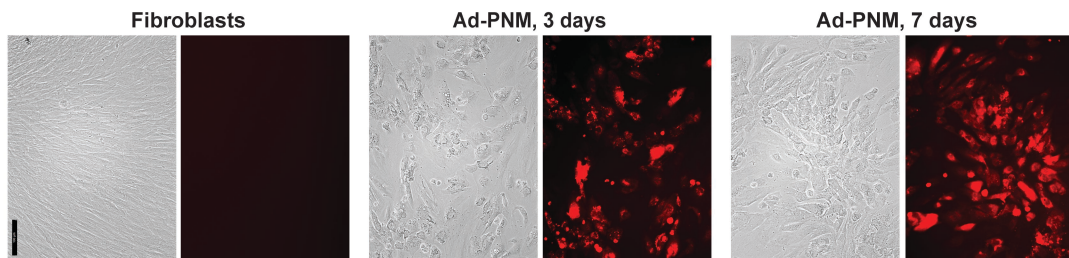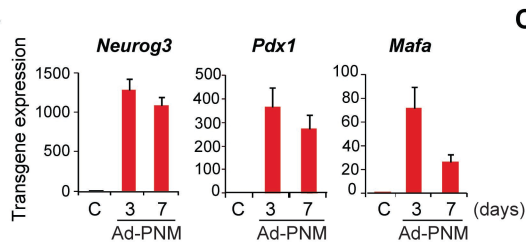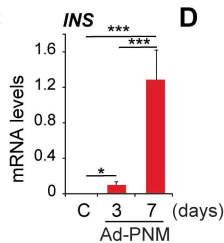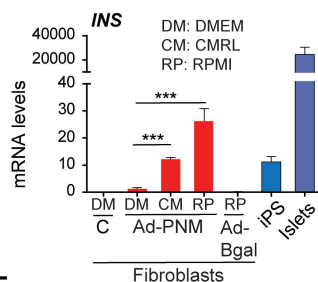
953   using unpaired t-test.

954

955

Figure 1

A
Fibroblasts | Ad-PNM, 3 days | Ad-PNM, 7 days

B Transgene expression — *Neurog3*, *Pdx1*, *Mafa* (C, 3, 7 days; Ad-PNM)

C *INS* — mRNA levels (C, 3, 7 days; Ad-PNM) *** *

D *INS* — mRNA levels (DM: DMEM, CM: CMRL, RP: RPMI); C, Ad-PNM, Ad-Bgal, iPS, Islets; Fibroblasts

E *NEUROD1*, *INSM1*, *PAX4*, *NKX2-2*, *ARX* — mRNA levels (C vs Ad-PNM)

F *GCG*, *SST* — mRNA levels (C vs Ad-PNM)

G mRNA levels — Fibroblasts (dashed line at 1.0); *TWIST2*, *PRRX1*, *LHX9*, *FOXF2*, *CD49A*, *CD29*, *P4H*, *COL1A1* (3, 7 days)

Figure 2

Figure 3

Figure 4

A

- No response
- Response to glucose and high K$^+$
- Response to high K$^+$
- Response to glucose

35 %
35 %
27 %
3 %

B

G2   G20   +KCl 30mM

0.25 (a.u)
100s

C

G2   G20   +KCl 30mM

0.5 (a.u)
100s

G2   G20   +KCl 30mM

1 (a.u)
100s

G2   G20   +KCl 30mM

0.5 (a.u)
100s

G2   G20   +KCl 30mM

0.25 (a.u)
100s

D

Human insulin (uU/100.000 cells)

Fibroblasts: 2, 20
5FT: 2, 20
mM

Figure 5

A

Ad-PNM   Ad-Pax4   Ad-Nkx2-2   collect

seed

-1 | 1 | 2 | 3 | 4 | 5 | 6 | 7 | 8 | 9 | 10 | 11   day

3D

B

C-peptide   Hoechst

C

mRNA levels (3D vs 2D)

INS NEUROD1 INSM1 NKX6-1 PAX6 MAFB PDX1 NGN3 PAX4 NKX2-2 PCSK1 PCSK2 ABCC8 KCNJ11 GIPR GLP1R CXCR4 IA2 NCAM1 CHGB

** *** *** ** *** **

0.07

Transcription   Function

D

Human insulin (uU/ 50 spheroids)

*

2   20   2   20   mM

Fibroblasts   iβ-like

E

Glucose stimulation index

***

2D   3D

iβ-like

F

Human insulin (uU/ 50 spheroids)

***

*

*

2   5   11   20

Glucose (mM)

G

Golgi

mit

N   ER   LD

Figure 6

A iβ-like cells spheroids — 300 — ACE, day 10, NSG mouse — 4000 — Subcutaneous / Omentum, day 15, day 30

B

C RITC-dextran / CFDA, z=33,0µm

D hTBP (relative mTbp); hINS (relative hTBP) — mRNA expression: non-transplanted, fibroblasts, iβ-like

E HLA / c-peptide / Merge

F C-peptide + / HLA + (%) — 10d

G Human insulin (mU/L) in aqueous humour — non-transplanted, fibroblasts, iβ-like, human islets — ***

H Human insulin (mU/L) in plasma — Subcutaneous, Omentum — non-transplanted, iβ-like, islets ACE

Supplemental information

for

DIRECT REPROGRAMMING OF HUMAN FIBROBLASTS INTO INSULIN-PRODUCING CELLS BY TRANSCRIPTION FACTORS

Marta Fontcuberta-PiSunyer, Ainhoa García-Alamán, Èlia Prades, Noèlia Téllez, Hugo Figueiredo, Rebeca Fernandez-Ruiz, Sara Cervantes, Carlos Enrich, Laura Clua, Javier Ramón-Azcón, Christophe Broca, Anne Wojtusciszyn, Anna Novials, Nuria Montserrat, Josep Vidal, Ramon Gomis, Rosa Gasa
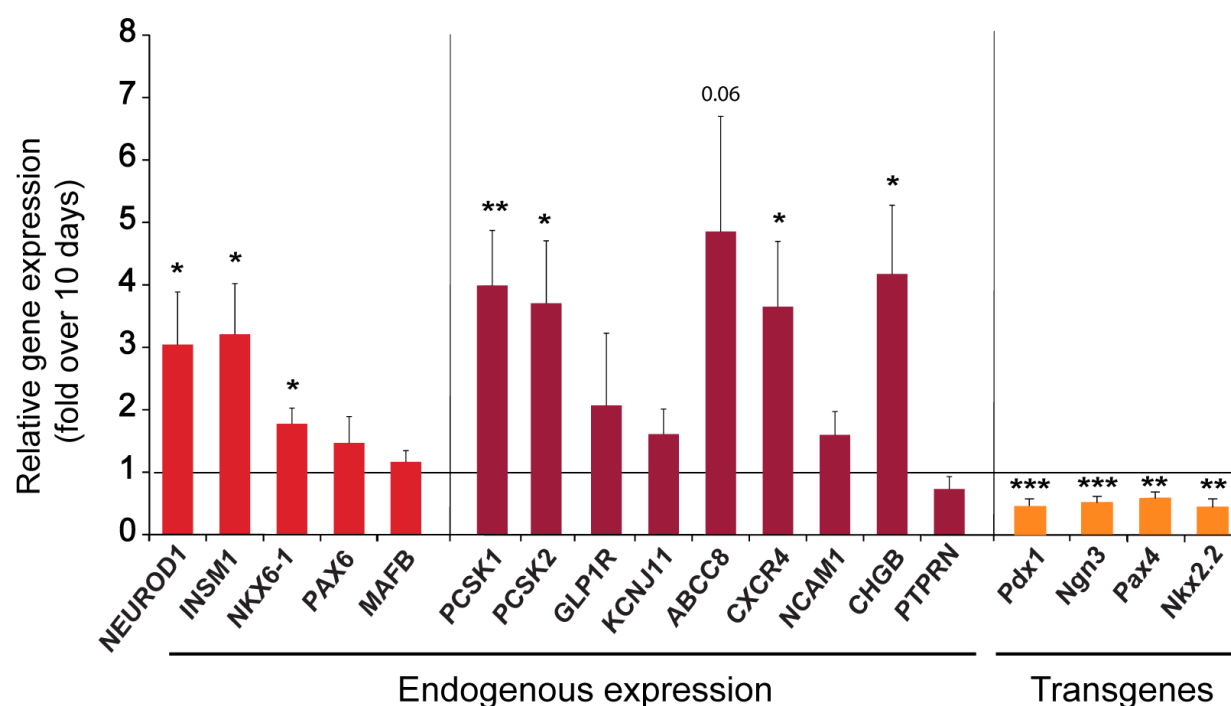
This document contains:

- Figures S1 to S6: pages 2-6
- Tables S1-S3: pages 7-11
- Video captions: page 12

	Bright field	**Cherry**
Control		
Ad-PNM		
Ad-PNM +superfect		
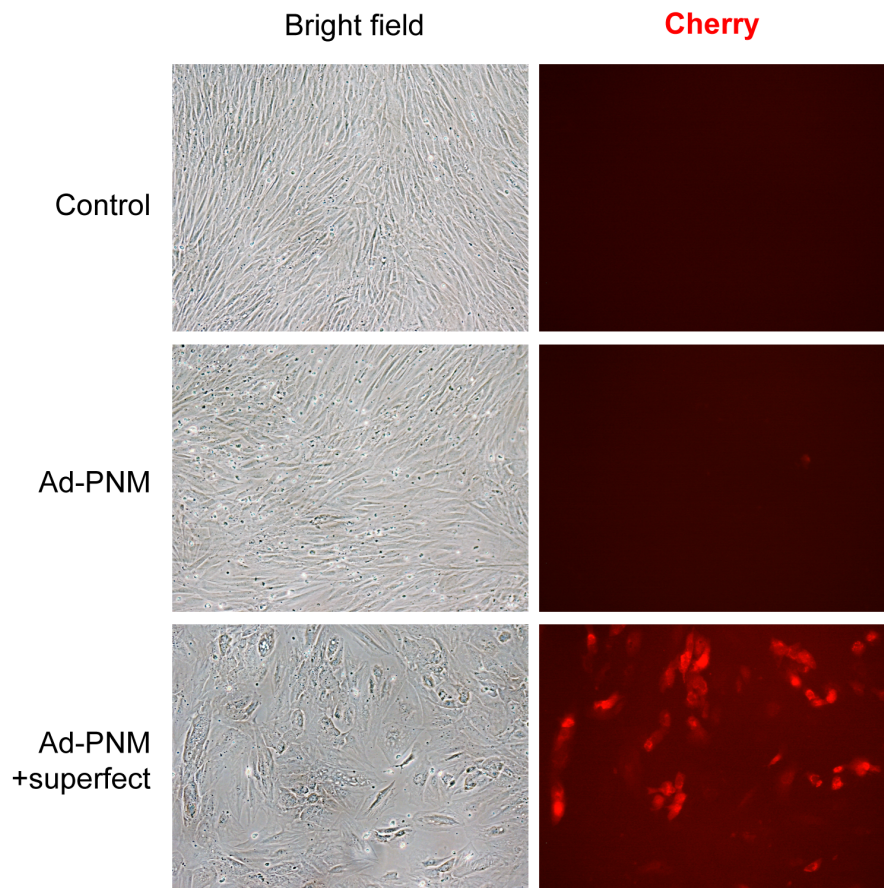
Supplementary S1. Human primary foreskin fibroblasts HFF1 were treated for 14h with a polycistronic recombinant adenovirus (Ad-PNM) encoding the PNM factors (Pdx1, Neurog3 and Mafa) and a Cherry reporter protein, in the presence or absence of the Superfect transfection reagent. Bright field and Cherry immunofluorescence images from control (parental) fibroblasts and HFF1 fibroblasts four days after infection.

A

B

Supplementary S2. (A) qRT-PCR for human *INS* in human foreskin fibroblasts HFF1 ten days after infection with the recombinant adenoviruses encoding the indicated transcription factors. All adenoviruses except Ad-PNM encoded a single transcription factor. Adenoviruses that were added simultaneously are shown in parenthesis. Order of addition is left to right. Expression levels were calculated relative to *TBP*. Data are mean ± SEM for n=2-9. **(B)** Real time amplification plots for *INS* and *TBP* in parental fibroblasts and in fibroblasts seven days after infection with Ad-PNM.

3

Supplementary S3: qRT-PCR of the indicated genes at day 21 after initiation of reprogramming. Transcript levels are expressed relative to levels in cells at day 10 of the reprogramming protocol (given the value of 1). Cells were maintained in 2D culture throughout the duration of the experiment. Data are mean ± SEM for n=9-13, from 7 reprogramming experiments. *P< 0.05, **P< 0.01, ***, P< 0.001, vs. iβ-cells at day10 using
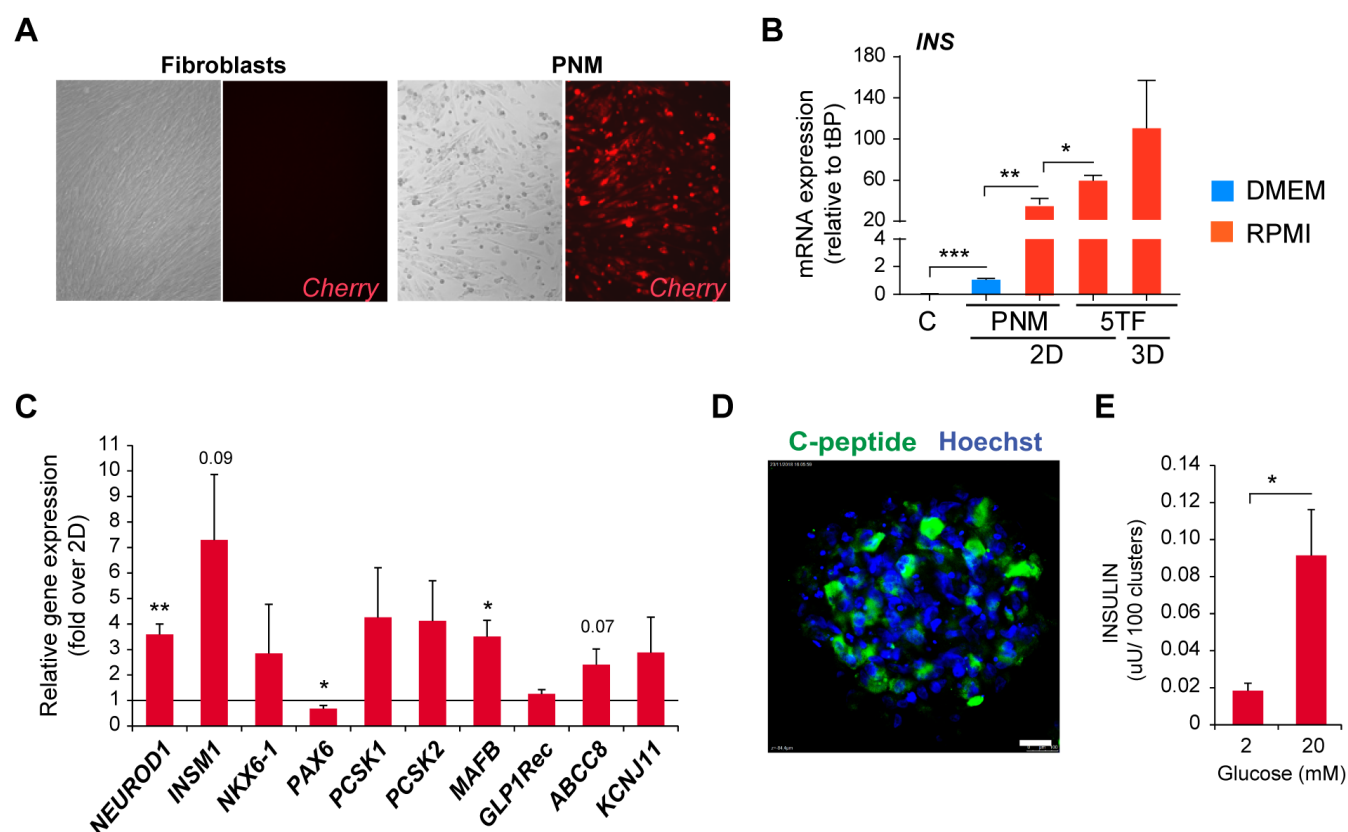
Supplementary S4: Human primary foreskin fibroblasts HFF2 were subjected to transcription factor-based reprogramming towards insulin-producing cells. **(A)** Bright field and Cherry immunofluorescence images from control (parental) fibroblasts and from fibroblasts three days after infection with Ad-PNM. Scale bar is 100 uM. **(B)** qRT-PCR for *INS* in HFF2 ten days after infection with Ad-PNM alone and cultured under 2D conditions in DMEM (blue) or RPMI-1640 media (red) (n=6), or subjected to the 5TF reprogramming protocol and cultured in RPMI-1640 media under 2D or 3D (n=4) conditions as indicated. Expression levels were calculated relative to *TBP*. Note that changes in *INS* gene expression in the different reprogramming conditions follow a similar trend as observed with HFF1 fibroblasts. **(C)** qRT-PCR of the indicated genes in HFF2-derived iβ-like cell spheroids (n=6) Transcript levels are expressed relative to HFF2-derived iβ-like cells maintained in 2D culture throughout the 10-day protocol (given the value of 1). **(D)** Representative immunofluorescence image showing C-peptide staining in green and nuclei in blue (marked with Hoechst). Scale bar is 100 μm. **(E)** In vitro glucose-induced insulin secretion by iβ-like cell spheroids. Data are calculated as mean ± SEM for 3 independent experiments, 1-3 replicates per experiment. *, P< 0.05; **, P< 0.01; ***, P< 0.001 relative to 2D in C using one-sample test, or between indicated conditions in B and E using unpaired t-test.

5

A

HLA C-peptide Hoechst

B

Nkx2-2 C-peptide **Pdx1 C-peptide** **Mafa C-peptide**
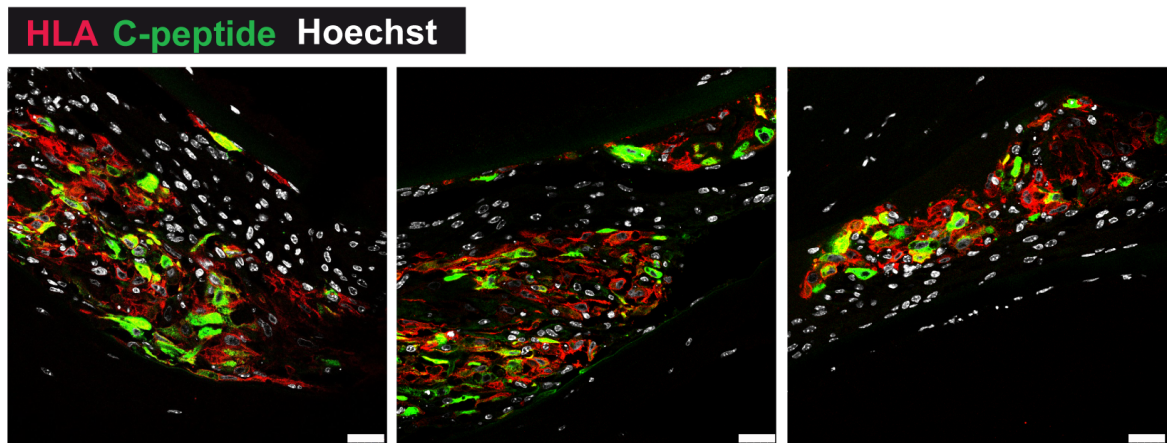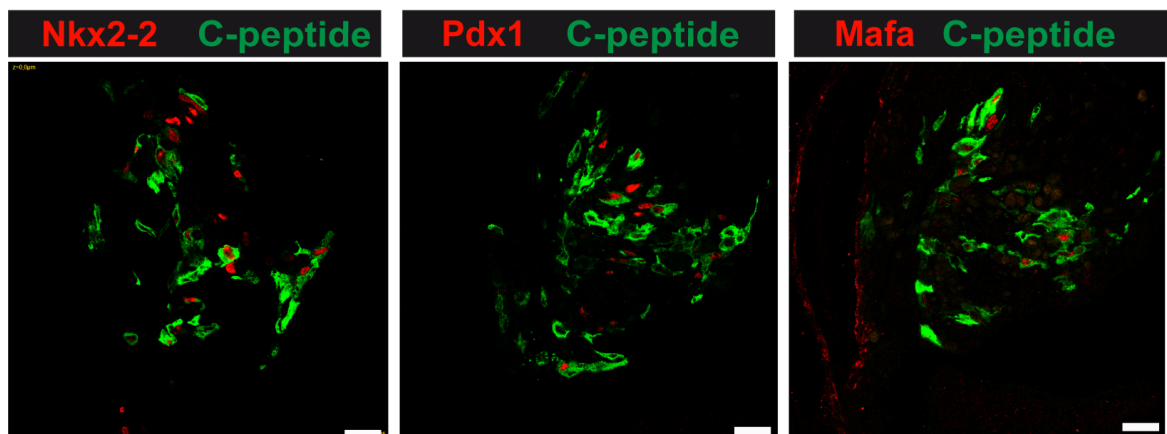
Supplementary S5: Immunostaining of iβ-cell spheroids ten days after their transplantation into the anterior chamber of the eye of NSG mice. Representative immunofluorescence images showing **(A)** C-peptide staining (green), HLA (red) and cell nuclei marked with Hoechst (white) and **(B)** C-peptide (green) with the indicated transcription factors (red). Scale bars are 25 μm.

Table S1. Comparison of gene expression levels between iβ-cells maintained in 2D culture, iβ-cell spheroids (3D) and human islets for the indicated genes. Fold expression values are calculated using qPCR data presented in Figures 1D&E, 2A, 3A-C and 5C.

Gene	Fold expression Islets/ iβ-cells 2D	Fold expression Islets/ iβ-cell 3D
ABCC8	2335	450
CHGB	23036	9251
CX36	3589	399
CXCR4	6	2
GIPR	10	6
GLP1R	163	100
INS	358	205
INSM1	134	41
KCNJ11	51	12
MAFB	8	4
NCAM1	2	2
NEUROD1	200	63
NEUROG3	2	3
NKX2-2	196	265
NKX6-1	117	37
PAX4	14	9
PAX6	425	327
PCSK1	16	5
PCSK2	81	48
PDX1	115	68
PTPRN (IA2)	30	25

7

Table S2. Comparison of circulating human insulin levels in transplanted mice between our study and several publications using stem cell-derived β-like cells.

Cells	Number of cells	Site	Days post-transplantation	Insulin (μU/ml)		Source
				basal	after glucose	
iβ-like cells	4 x 10^6	Subcutaneous	day 15	0.18-0.24	0.57-1.67	our study
			day 30	0-0.71	0.33-2.36	
iβ-like cells	4 x 10^6	omentum	day 15	0-0.63	0-5.24	our study
			day 30	0-5.2	2.36-5.23	
hES-derived endoderm	15 x 10^6	epididymal fat	day 94	13-36	56-110	Kroon et al. Nature Biotech 26, 443-452, 2008
hES-derived (PH, original differentation protocol)	5 x 10^6	kidney capsule	day 15	0-0.5	0-1	Pagliuca et al. Cell 159, 428-439, 2014
hES-derived SC-β cells (optimized protocol)	5 x 10^6	kidney capsule	day 15	1-5	1-11	
hiPSC-derived SC-β cells (optimized protocol)	5 x 10^6	kidney capsule	day 15	5	7.5	Millman et al. Nat Commun 7, 11463, 2016
hES-derived SC-β cells (optimized protocol)	5 x 10^6	kidney capsule	day 180	11	23	Velazco-Cruz et al. Stem cell Reports 12, 351-365, 2019

8

Table S3. List of oligonucleotides used for real time PCR.

Gene	Species	Primer ID	Primer sequence (5' to 3')
ABCC8	human	*Forward*	AGACCCTCATGAACCGACAG
ABCC8	human	*Reverse*	GGCTCTGTGGCTTTTCTCTC
ARX	human	*Forward*	GCAAGGAGGTGTGCTAAAGG
ARX	human	*Reverse*	GGAGTGTGCTGGTCCTCTGT
CD29	human	*Forward*	CAAAGGAACAGCAGAGAAGC
CD29	human	*Reverse*	ATTGAGTAAGACAGGTCCATAAGG
CD49a	human	*Forward*	GCTGGCTCCTCACTGTTGTT
CD49a	human	*Reverse*	CTCCATTTGGGTTGGTGACT
CHGB	human	*Reverse*	TTGGATGTCCTCCTCCCCTG
CHGB	human	*Forward*	CGCCAAGTCCTGAAGACGA
COL1A1	human	*Forward*	CTCGAGGTGGACACCACCCT
COL1A1	human	*Reverse*	CAGCTGGATGGCCACATCGG
CX36	human	*Forward*	GCAGCAGCACTCCACTATGA
CX36	human	*Reverse*	TACACCGTCTCCCCCACAAT
CXCL12	human	*Forward*	GAGCCAACGTCAAGCATCTC
CXCL12	human	*Reverse*	AGCTTCGGGTCAATGCACA
CXCR4	human	*Forward*	CGTCTCAGTGCCCTTTTGTTC
CXCR4	human	*Reverse*	CTGAAGTAGTGGGCTAAGGGC
FOXF2	human	*Forward*	CTACTTGCACCAGAACGCTC
FOXF2	human	*Reverse*	CGCAGGGCTTAATATCCTGACA
GCG	human	*Forward*	CACAGGGCACATTCACCAG
GCG	human	*Reverse*	TCTGGGAAATCTCGCCTTCC
GIPR	human	*Forward*	ACAATGTGAGAACCCAGAGAAG
GIPR	human	*Reverse*	CGCCTGAACAAACTCAAGATG
GLP1R	human	*Forward*	TTCTCTGCTCTGGTTATCGCC
GLP1R	human	*Reverse*	GGATGCAAACAGGTTCAGGT
HNF1B	human	*Forward*	ACCAAGCCGGTCTTCCATACT
HNF1B	human	*Reverse*	GGTGTGTCATAGTCGTCGCC
IGFBP4	human	*Forward*	TGTTGCACCATCTGCTTGGT
IGFBP4	human	*Reverse*	ATGTACCCCACCTCCCTAGC
INS	human	*Forward*	GCAGCCTTTGTGAACCAACA
INS	human	*Reverse*	TTCCCCGCACACTAGGTAGAGA
INSM1	human	*Forward*	TTTTGGAACCCCCACTTTTAC
INSM1	human	*Reverse*	CGAGACCAGACCGCATTT
KCNJ11	human	*Forward*	TGTGTCACCAGCATCCACTC
KCNJ11	human	*Reverse*	CACTTGGACCTCAATGGAGAA
LDHA	human	*Forward*	GCAAGAGGGAGAAAGCCGTC
LDHA	human	*Reverse*	CTTCCAAGCCACGTAGGTCA
LHX9	human	*Forward*	TGCCAAGGACGGTAGCATTT

9

LHX9	human	*Reverse*	GCAGCTCAGGTGGTAGACAG
MafA	mouse	*Forward*	CTTCAGCAAGGAGGAGGTCA
MafA	mouse	*Reverse*	TTGTACAGGTCCCGCTCTTT
MAFB	human	*Forward*	AACTTTGTCTTGGGGCACAC
MAFB	human	*Reverse*	GGGACCTCTCGGTTCTCTCT
MCT1 (SLC16A1)	human	*Forward*	CACCAGCGAAGTGTCATGGA
MCT1 (SLC16A1)	human	*Reverse*	ATCAAGCCACAGCCTGACAA
MYT1	human	*Forward*	AGTGTCTGCCCAGGTGTCTT
MYT1	human	*Reverse*	GACAGACAATAGCTGTGGGGA
NCAM 1	human	*Forward*	CCTCCCAGCCAGCAGATTAC
NCAM1	human	*Reverse*	CTCTCCAACGCTGATCTCCC
NEUROD1	human	*Forward*	AGGAAGAAGAGGAAGAGGAGGATG
NEUROD1	human	*Reverse*	TTGGTGGTGGGTTGGGATAAG
NEUROG3	human	*Forward*	AGACGACGCGAAGCTCACC
NEUROG3	human	*Reverse*	AAGCCAGACTGCCTGGGCT
Neurog3	mouse	*Forward*	CCCACCTAGCCCCACTCTCATACC
Neurog3	mouse	*Reverse*	CGCCGGCTTCTTCGCTGTTT
NKX2.2	human	*Forward*	CTTCTACGACAGCAGCGACAACCCG
NKX2.2	human	*Reverse*	CCTTGGAGAAAAGCACTCGCCGCTTT
NKX6-1	human	*Forward*	ACACGAGACCCACTTTTTCCG
NKX6-1	human	*Reverse*	GCCCCGCCAAGTATTTTGTT
OAT	human	*Forward*	CGTAAGTGGGGCTATACCGT
OAT	human	*Reverse*	CTGGTTGGGTCTGTGGAACT
P4H	human	*Forward*	TCGAGTTCACCGAGCAGACA
P4H	human	*Reverse*	GAACAGCAGGATGTGAGTCTTGA
PAX4	human	*Forward*	AGCAGAGGCACTGGAGAAAGAGTT
PAX4	human	*Reverse*	CAGCTGCATTTCCCACTTGAGCTT
PAX6	human	*Forward*	AGACACAGCCCTCACAAACA
PAX6	human	*Reverse*	ATCATAACTCCGCCCATTCA
PCSK1	human	*Forward*	AAGCAAACCCAAATCTCACCTGGC
PCSK1	human	*Reverse*	TCACCATCAAGCCTGCTCCATTCT
PCSK2	human	*Forward*	CCGGGTTCCTCTTCTGTGTC
PCSK2	human	*Reverse*	AGCAAAGGGAAGCTTTCGGA
PDGFRA	human	*Forward*	TGTGGGACATTCATTGCGGA
PDGFRA	human	*Reverse*	AAGCTGGCAGAGGATTAGGC
PDX1	human	*Forward*	CCCATGGATGAAGTCTACC
PDX1	human	*Reverse*	GTCCTCCTCCTTTTTCCAC
Pdx1	mouse	*Forward*	CCCCAGTTTACAAGCTCGCT
Pdx1	mouse	*Reverse*	CTCGGTTCCATTCGGGAAAGG
PRRX1	human	*Forward*	CGAGAGTGCAGGTGTGGTTT

PRRX1	human	*Reverse*	GAGCAGGACGAGGTACGATG
REST	human	*Forward*	CTCATACAGGAGAACGCCCA
REST	human	*Reverse*	GAGGCCACATAACTGCACTG
PTPRN (IA2)	human	*Reverse*	GGTGGAGGATGGTGTCAAGC
PTPRN (IA2)	human	*Forward*	AAGCTCCGCACCAGAAAGTC
SMAD3	human	*Forward*	CATCGAGCCCCAGAGCAATA
SMAD3	human	*Reverse*	TTTGGAGAACCTGCGTCCAT
SST	human	*Forward*	CAGTTTCTGCAGAAGTCCCTG
SST	human	Reverse	AATTCTTGCAGCCAGCTTTGC
TBP	human	*Forward*	ATCCCTCCCCCATGACTCCCATG
TBP	human	*Reverse*	ATGATTACCGCAGCAAACCGC
Tbp	mouse	*Forward*	ACCCTTCACCAATGACTCCTATG
Tbp	mouse	*Reverse*	ATGATGACTGCAGCAAATCGC
TBP	human(specific)	*Forward*	TGTGCTCACCCACCAACAAT
TBP	human(specific)	*Reverse*	ACGTCGTCTTCCTGAATCCC
TWIST2	human	*Forward*	CGCAAGTGGAATTGGGATGC
TWIST2	human	*Reverse*	CGATGTCACTGCTGTCCCTT

VIDEO CAPTIONS

Video S1

Video shows changes in fluorescence of an isolated iβ-like cell in response to high glucose (20mM) and high potassium (KCl 30mM). Cell had been pre-loaded with the calcium indicator Fluo-2. Video was recorded using a Leica TCS SPE confocal microscope with an incubation chamber set at 37°C, and a 40X oil immersion objective.

Video S2

Video shows fluorescence of parental fibroblasts HFF1 in response to high glucose (20mM) and high potassium (KCl 30mM). Cells had been pre-loaded with the calcium indicator Fluo-2. Note that fibroblasts exhibit no changes in fluorescence in response to the tested stimuli. Video was recorded using a Leica TCS SPE confocal microscope with an incubation chamber set at 37°C, and a 40X oil immersion objective.